

Calcium Absorption by Fish Intestine: The Involvement of ATP- and Sodium-Dependent Calcium Extrusion Mechanisms

Gert Flik, Theo J.M. Schoenmakers, Jack A. Groot†, Carel H. van Os‡, and Sjoerd E. Wendelaar Bonga

Department of Animal Physiology, Faculty of Science, University of Nijmegen, 6525 ED Nijmegen, The Netherlands,

†Department of Animal Physiology, University of Amsterdam, 1098 SM Amsterdam, The Netherlands, ‡Department of Physiology, Faculty of Medicine, University of Nijmegen, 6500 HB Nijmegen, The Netherlands

Summary. Measurements of unidirectional calcium fluxes in stripped intestinal epithelium of the tilapia, *Oreochromis mossambicus*, in the presence of ouabain or in the absence of sodium indicated that calcium absorption via the fish intestine is sodium dependent. Active Ca^{2+} transport mechanisms in the enterocyte plasma membrane were analyzed. The maximum capacity of the ATP-dependent Ca^{2+} pump (V_m : $0.63 \text{ nmol} \cdot \text{min}^{-1} \cdot \text{mg}^{-1}$, K_m : 27 nM Ca^{2+}) is calculated to be $2.17 \text{ nmol} \cdot \text{min}^{-1} \cdot \text{mg}^{-1}$, correcting for 29% inside-out oriented vesicles in the membrane preparation. The maximum capacity of the $\text{Na}^+/\text{Ca}^{2+}$ exchanger with high affinity for Ca^{2+} (V_m : $7.2 \text{ nmol} \cdot \text{min}^{-1} \cdot \text{mg}^{-1}$, K_m : 181 nM Ca^{2+}) is calculated to be $13.6 \text{ nmol} \cdot \text{min}^{-1} \cdot \text{mg}^{-1}$, correcting for 53% resealed vesicles and assuming symmetrical behavior of the $\text{Na}^+/\text{Ca}^{2+}$ exchanger. The high affinity for Ca^{2+} and the sixfold higher capacity of the exchanger compared to the ATPase suggest strongly that the $\text{Na}^+/\text{Ca}^{2+}$ exchanger will contribute substantially to Ca^{2+} extrusion in the fish enterocyte. Further evidence for an important contribution of $\text{Na}^+/\text{Ca}^{2+}$ exchange to Ca^{2+} extrusion was obtained from studies in which the simultaneous operation of ATP- and Na^+ -gradient-driven Ca^{2+} pumps in inside-out vesicles was evaluated. The fish enterocyte appears to present a model for a Ca^{2+} transporting cell, in which $\text{Na}^+/\text{Ca}^{2+}$ exchange activity with high affinity for Ca^{2+} extrudes Ca^{2+} from the cell.

Key Words $(\text{Na}^+ + \text{K}^+)\text{-ATPase}$ · $(\text{Ca}^{2+} + \text{Mg}^{2+})\text{-ATPase}$ · $\text{Na}^+/\text{Ca}^{2+}$ exchange · enterocyte · plasma membrane · teleost fish · tilapia · bepridil

Introduction

Freshwater fish depend on two routes for the uptake of calcium, *viz.* via their gills and via their gut. Direct absorption of Ca^{2+} from the water via the gills may provide for up to 94% of the total calcium required [10]. However, at decreased calcium availability in the water (e.g., in very soft freshwater) or in times of increased need for calcium (e.g., during gonadal maturation) enhanced intestinal calcium

absorption may compensate for insufficient extraintestinal calcium absorption [4].

In mammalian Ca^{2+} transporting epithelia such as the duodenum and renal tubules ATP-dependent Ca^{2+} transport is regarded the predominant mode of Ca^{2+} extrusion across basolateral membranes by which transcellular transport of Ca^{2+} is achieved [16, 19, 20]. However, the presence of a $\text{Na}^+/\text{Ca}^{2+}$ exchanger in the same plasma membrane has raised questions about the relative contribution of both mechanisms to Ca^{2+} extrusion. The affinity for Ca^{2+} and the maximum transport capacity of the $(\text{Ca}^{2+} + \text{Mg}^{2+})\text{-ATPase}$, determined *in vitro*, are generally much higher than these values for the $\text{Na}^+/\text{Ca}^{2+}$ exchanger. Therefore, the role of $\text{Na}^+/\text{Ca}^{2+}$ exchange in transcellular Ca^{2+} transport in mammalian intestinal and renal epithelia appears of minor importance [24, 36].

In recent studies on transport mechanisms in fish gills [13, 14, 26] we demonstrated that branchial transepithelial calcium transport depends on a $(\text{Ca}^{2+} + \text{Mg}^{2+})\text{-ATPase}$ mediated extrusion of Ca^{2+} over the basolateral membranes of the calcium transporting cells. We report here on intestinal Ca^{2+} uptake of a freshwater fish, the teleost *Oreochromis mossambicus* (hereafter called tilapia), which process in contrast appears Na^+ dependent and is correlated with a powerful $\text{Na}^+/\text{Ca}^{2+}$ exchange activity in the basolateral plasma membrane of the enterocyte.

Materials and Methods

Male tilapia, *Oreochromis mossambicus*, with an average body weight of 250 g were obtained from laboratory stock, kept in 100 liter aquaria supplied with running tapwater (0.7 mM Ca , 26°C) under a photoperiod of 16 hr of light alternating with 8 hr of

darkness. The fish were fed Tetramin® tropical fish food, 1.5 % body weight per day; feeding was discontinued one day before experimentation. Fish were anesthetized in tricaine methanesulphate (3 g · liter⁻¹, adjusted to pH 7.4 with Tris) and killed by spinal transection. The peritoneal cavity was opened and the intestinal tract removed. In all experiments the proximal $\frac{1}{3}$ part of the intestine was used (approximately 30 cm; this part shows no macroscopically or (sub)microscopically distinct transitions in epithelial make-up; *personal observations*). The intestine was rapidly flushed with saline and processed as described below.

TRANSEPITHELIAL Ca²⁺ TRANSPORT

Mucosa of the proximal 10 cm of the intestine was stripped of underlying muscle layers and mounted in Ussing chambers for transepithelial flux measurements, as described in detail for goldfish intestinal mucosa [2]. All flux experiments were carried out at 23°C. In short, tissue was mounted in slides and preincubated for 30 min in gassed saline (117.5 mM NaCl, 5.7 mM KCl, 25 mM NaHCO₃, 1.2 mM NaH₂PO₄, 1.25 mM CaCl₂, 1.2 mM MgSO₄ and 28 mM mannitol, 95% O₂/5% CO₂, pH 7.3 ± 0.1). Next, the slides were mounted as the partition between two 3 ml half-chambers filled with saline. The exposed tissue area was 0.2 cm². At zero time ⁴⁵CaCl₂ (specific activity: 180 MBq · mmol⁻¹) was added as tracer to either side of the tissue. After 30 min, samples (100 µl) were taken from both half-chambers simultaneously every 15 min, for a total period of 150 min. In pilot experiments it was established that unidirectional fluxes are constant over this time period. Ouabain (0.1 mM) was added at $t = 90$ min to the serosal side of the epithelium. In 'sodium-free' media, NaCl was replaced by N-methyl-D-glucamine chloride (NMGC1), NaH₂PO₄ by KH₂PO₄ and NaHCO₃ by Tris/HEPES (pH 7.3). Unidirectional steady-state Ca²⁺ fluxes were determined over 15-min periods and for each tissue sample an average value was calculated for $t = 30$ to 90 min (control period) and $t = 90$ to 150 min (ouabain present), to calculate ouabain sensitivity of individual tissue samples. Flux values during the first 15 min after addition of ouabain did not differ significantly from the values obtained during the subsequent two 15-min periods. To calculate net fluxes, values for unidirectional fluxes from mucosa to serosa (J_{ms}) and from serosa to mucosa (J_{sm}) across adjacent segments from the same fish were used in data analysis. Ca²⁺ fluxes were expressed in nmol · h⁻¹ · cm⁻².

ISOLATION OF BASOLATERAL PLASMA MEMBRANES

All steps were performed at 0–4°C. The proximal $\frac{1}{3}$ of the intestine was flushed with ice-cold saline (150 mM NaCl, 1 mM HEPES/Tris at pH 8.0, 1 mM DTT, 0.1 mM EDTA), cut lengthwise and rinsed thoroughly with the same saline. Next, the mucosa was collected by scraping with a microscope slide. Scrapings were disrupted with a dounce homogenizer equipped with a loosely fitting pestle (25 strokes) in isotonic buffer (250 mM sucrose, 10 mM HEPES/Tris at pH 8.0, 1 mM DTT, 100 U · ml⁻¹ aprotinin; 1 g wet wt tissue per 20-ml buffer). The homogenate was centrifuged for 10 min at 1400 × g_{av} (Beckman TJ-6R, TH-4 rotor, 2800 rpm) to remove nuclei and cellular debris. Membranes were collected by centrifugation for 25 min at 150,000 × g_{av} (Beckman L8-80, 70Ti rotor, 45,000 rpm). The pellet thus obtained consisted of a brownish part well-fixed to the wall of the

tube and a fluffy layer on top. The brownish part contained roughly 90% of the total succinic acid dehydrogenase (SDH) activity of the tissue. The fluffy part of the pellet was removed by shaking mildly and resuspended (100 strokes) in a dounce homogenizer fitted with a loosely fitting pestle in 10 ml (for material obtained from one fish of 250 g) isotonic buffer (250 mM sucrose, 10 mM HEPES/Tris at pH 7.4, 100 U · ml⁻¹ aprotinin). This homogenate was brought to 37% (wt/wt) sucrose by mixing (five strokes) with 1.25 volumes sucrose (60% wt/wt) in 10 mM HEPES/Tris (pH 7.4). Eight ml of this suspension was covered with 4 ml isotonic sucrose and centrifuged isopycnicly for 90 min at 200,000 × g_{av} (Beckman SW 40 Ti rotor, 40,000 rpm). The membranes at the interface of the sucrose block and the isotonic buffer were collected (approximately 0.5 ml) and mixed with 13 ml isotonic buffer, containing the basic ingredients of the assay medium (150 mM NaCl or KCl, 20 mM HEPES/Tris, pH 7.4, and 0.8 mM MgCl₂; further called assay buffer). The membranes were pelleted by centrifugation, 35 min at 180,000 × g_{av} (SW 40Ti, 38,000 rpm). The pellet was rinsed twice with assay buffer and resuspended by 25 passages through a 23-G needle in 0.5–1.0 ml assay buffer. The assay buffer contained either NaCl or KCl depending on the subsequent assays. Typically, the membrane preparations contained 5 mg · ml⁻¹ protein and were used on the day of isolation without being frozen (protein recovery was 2.52 ± 0.68%, $n = 21$).

ENZYME ASSAYS

Protein was determined with a commercial reagent kit (Biorad), using bovine serum albumin (BSA) as reference. The marker enzymes used to characterize the membrane preparations were: (Na⁺ + K⁺)-ATPase for basolateral plasma membranes, alkaline phosphatase (APase, determined at pH 10.4) for brush-border membranes, succinic acid dehydrogenase (SDH) for mitochondrial membrane fragments and thiamine pyrophosphatase (TPPase) for Golgi membranes; assay conditions have been described in detail elsewhere [14]. Maximum enzymic activities were obtained after preincubation (10 min at 37°C) with detergent at optimum concentration: 0.2 mg · ml⁻¹ saponin was used at a protein concentration of 1 mg · ml⁻¹. Data on recovery and purification of marker enzymes are given in Table 1. The final membrane fraction used for transport studies was enriched 9.3-fold in the basolateral membrane marker (Na⁺ + K⁺)-ATPase compared to the homogenate. The (Na⁺ + K⁺)-ATPase specific activity averaged 169 ± 36 ($n = 9$) µmol P_i · hr⁻¹ · mg⁻¹ at 37°C. APase, SDH, and TPPase activities were not enriched. To exclude possible contributions of enzymic activities from mitochondrial membrane contamination, routinely 5 µg · ml⁻¹ oligomycin B was included in Ca²⁺ transport assay media. Ruthenium red (10 µM) did not influence kinetics of ATP-driven Ca²⁺ transport in our membrane preparations (*results not shown*).

VESICULAR SPACE AND MEMBRANE ORIENTATION

Uptake of D-(¹⁴C)-mannitol (Amersham) in membrane vesicles was determined in a Ca²⁺ transport medium (1 µM Ca²⁺, no ⁴⁵Ca) made 100 µM in mannitol to which 7.6 × 10⁵ Bq · ml⁻¹ ¹⁴C-mannitol had been added. The vesicular space calculated on the basis of vesicle mannitol content at equilibrium after 2 hr of incubation ranged from 2.75 to 3.25 µl · mg⁻¹, a value comparable to that reported for rat ileal plasma membrane vesicles [16].

The percentage inside-out oriented resealed vesicles (IOV's) was determined on the basis of acetylcholine esterase

Table 1. Relative recoveries and enrichment of marker enzymes in tilapia enterocyte plasma membranes

	Recovery (%) ^a	Enrichment ^b
Protein	2.5 ± 0.7(21)	—
Alkaline phosphatase	3.1 ± 1.3 (7)	0.92 ± 0.57(7)
Succinic acid dehydrogenase	3.0 ± 1.2 (9)	1.37 ± 0.45(9)
Thiamine pyrophosphatase	7.0 ± 3.1 (4)	1.50 ± 1.00(4)
Na ⁺ /K ⁺ -ATPase	23.1 ± 3.5 (8)	9.30 ± 2.40(8)

^a Recovery was calculated as the percentage total activity (equals specific activity · total protein) in the plasma membrane fraction relative to that in the initial homogenate.

^b Enrichment is the ratio of specific activities in the plasma membrane fraction and in the initial homogenate.

^c Numbers in parentheses indicate *n*.

latency of the membrane preparations [13]. The latent activity of this exoenzyme unmasked by saponin treatment (0.2 mg · (mg protein)⁻¹) reflected 29 ± 4% (*n* = 8) inside-out oriented vesicles in the preparation.

The percentage right-side-out oriented vesicles (ROV's) was determined on the basis of the specific trypsin sensitivity of the cytosol-oriented part of the (Na⁺ + K⁺)-ATPase. Following trypsin treatment, which inactivates (Na⁺ + K⁺)-ATPase in IOV's and leaky membrane fragments, latent (ROV) (Na⁺ + K⁺)-ATPase activity was unmasked by saponin treatment. The optimal trypsin (Sigma porcine trypsin, T0134) effect was obtained at 4500 BAEE units trypsin per mg membrane protein for 30 min at 25°C. Trypsin activity was quenched by the addition of 25 mg · ml⁻¹ soybean trypsin inhibitor (Sigma T9253). In controls the inhibitor was added before the addition of trypsin. The trypsin-insensitive (Na⁺ + K⁺)-ATPase activity in our membrane preparation amounted to 24 ± 5% of the total activity, indicating 24% ROV's. The membrane configuration of the plasma membrane preparation therefore is 29% IOV, 24% ROV and 47% leaky fragments. The 53% resealed membranes deduced from the percentages of IOV's and ROV's is congruous with a 45 ± 12% (*n* = 8) resealing as determined by saponin-unmasked Na⁺/K⁺-ATPase latency of the preparation.

VESICLE Ca²⁺ TRANSPORT

ATP-Dependent Transport

ATP-dependent transport of Ca²⁺ was assayed by means of a rapid filtration technique [19]. The composition of the assay medium was: 20 mM HEPES/Tris (pH 7.4), 3 mM Tris-ATP, 150 mM KCl, 0.8 mM free Mg²⁺, 7.5 × 10⁻⁵ to 10⁻³ mM free Ca²⁺, 0.5 mM EGTA, 0.5 mM N-(2-hydroxyethyl)-ethylenediamine-N,N',N'-triacetic acid (HEEDTA), 0.5 mM nitrilotriacetic acid (NTA), 5 μg · ml⁻¹ oligomycin B. The ⁴⁵Ca (specific activity 24 GBq · mmol⁻¹) radioactive concentration in the transport media ranged from 0.5 to 0.8 MBq · ml⁻¹. Incubations were carried out at 37°C, the optimum temperature of the ATPase. When oxalate (20 mM) was included in the assay media, Ca²⁺ complexed by oxalate was taken into account. The Ca²⁺ ionophore A23187 was dissolved in DMSO and added to the incubates at 5 μg · ml⁻¹, not exceeding 0.1% (vol/vol) DMSO. In some experiments calmodulin was added to the membranes (50

μg · mg⁻¹) and allowed to incubate for 30 min on ice before assay. The reaction was quenched by addition of 1 ml ice-cold stop buffer (150 mM KCl, 20 mM HEPES/Tris, pH 7.4, 0.1 mM LaCl₃) and the quenched sample filtered (Schleicher & Schuell ME25, pore size: 0.45 μm). The filters were rinsed twice with 2 ml of the same buffer. The amount of membrane protein per filter was 10 to 20 μg. The filters were dissolved in 4 ml Aqualuma® scintillation fluid (30 min at room temperature) and radioactivity was determined in a LKB rackbeta liquid scintillation analyzer.

Na⁺-Dependent Transport

Na⁺-dependent Ca²⁺ transport across plasma membranes was assayed as the difference in ⁴⁵Ca²⁺ accumulation upon transfer of membrane vesicles equilibrated in 150 mM NaCl to media containing either 150 mM NaCl (blank) or 150 mM KCl. To evaluate the sodium concentration dependence of ⁴⁵Ca²⁺ accumulation, vesicle suspensions were prepared in buffer with varying sodium concentrations replacing KCl for NaCl to maintain 150 mM of the combined salts. In composing the media, a 25-fold dilution of the vesicle suspension was taken into account to yield the following final concentrations: 150 mM NaCl and/or KCl, 20 mM HEPES/Tris (pH 7.4), 0.5 mM EGTA, 0.5 mM HEEDTA, 0.5 mM NTA, 0.8 mM free Mg²⁺, and 7.5 × 10⁻⁵ to 5 × 10⁻² mM free Ca²⁺. The ⁴⁵Ca radioactive concentration was 0.5 to 0.8 MBq · ml⁻¹. A 5-μl vesicle suspension was mixed with 120 μl medium. After 5 sec of incubation the reaction was quenched by addition of 1 ml stop buffer (150 mM NaCl, 20 mM HEPES/Tris at pH 7.4, 1.0 mM LaCl₃; 0°C) to the incubate. The membrane vesicles with retained ⁴⁵Ca were collected by filtration as described above. The Ca²⁺ ionophore A23187 and bepridil were dissolved in DMSO, the Na⁺-ionophore monensin and the K⁺-ionophore valinomycin in ethanol. The effects of ionophores and bepridil were evaluated by comparison with solvent treatment, not exceeding 0.1% (vol/vol) solvent in the incubate. Vesicles were preincubated with monensin and valinomycin, 10 min on ice. Bepridil was always freshly dissolved (stocks in DMSO proved instable).

To evaluate the relative contribution of Na⁺-gradient-driven and ATP-driven Ca²⁺ transport in plasma membrane vesicles, part of the KCl (150 mM, at 0 mM NaCl) in the ATPase assay medium was replaced by NaCl (5, 10, 15, 20, 25, 30 and 50 mM). By doing so, stimulation of (Na⁺ + K⁺)-ATPase activity in IOV's will result in Na⁺ loading of the IOV's and create a Na⁺ gradient to drive Ca²⁺ uptake into these vesicles on top of the ATP-driven Ca²⁺ uptake. Where indicated, vesicles were preincubated with ouabain for 2 hr on ice before Ca²⁺ uptake studies to prevent (Na⁺ + K⁺)-ATPase-mediated accumulation of Na⁺.

CALCULATIONS AND STATISTICS

Free Ca²⁺ and Mg²⁺ levels were calculated according to van Heeswijk et al. [19] and were based on the stability constants of the ligands EGTA, HEEDTA, NTA, ATP and oxalate given by Sillen and Martel [33]. The first and second protonations of the ligands were taken into account. The Ca²⁺ concentration dependence of ATP-dependent Ca²⁺ transport strictly obeyed Michaelis-Menten kinetics and data were analyzed accordingly. The Ca²⁺ concentration dependence of Na⁺-dependent Ca²⁺ transport did not obey simple Michaelis-Menten kinetics. The data were fitted according to:

$$V = (V'_m \cdot S)/(K'_m + S) + (V''_m \cdot S)/(K''_m + S) \quad (1)$$

Table 2. Ca^{2+} fluxes in stripped intestinal epithelium of the tilapia

	J_{ms}	J_{sm}	J_{net}
Control	$81 \pm 7(18)$	$47 \pm 4(18)$	$34 \pm 8(18)$
Ouabain	$64 \pm 5(18)^*$	$48 \pm 4(18)$	$16 \pm 6(18)^*$
NMG-Cl	$48 \pm 5(5)^*$	ND	
NMG-Cl + ouabain	$49 \pm 6(5)^*$	ND	

* $P < 0.001$, significantly different from control values. ND: Not determined. Numbers in parentheses indicate the number of experiments. J is expressed in $\text{nmol} \cdot \text{hr}^{-1} \cdot \text{cm}^{-2}$; J_{ms} : mucosa-to-serosa flux; J_{sm} : serosa-to-mucosa flux; $J_{net} = J_{ms} - J_{sm}$. Mean values \pm SE are given.

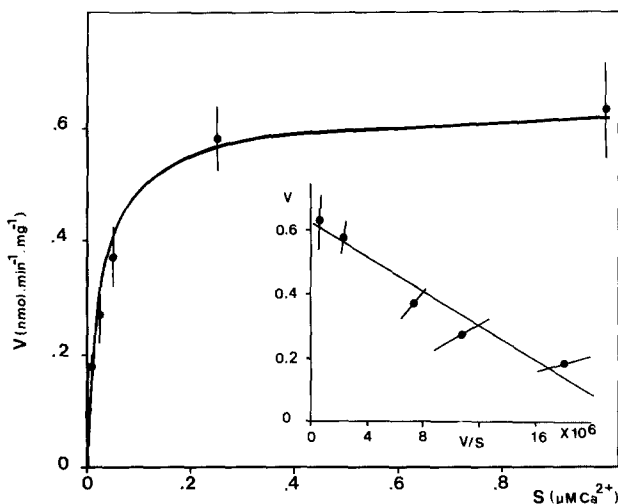


Fig. 1. Kinetics of ATP-dependent Ca^{2+} uptake in basolateral plasma membrane vesicles of tilapia enterocytes. Mean values for 12 different preparations are given. Initial rates of ATP-dependent Ca^{2+} uptake were corrected for ATP-independent uptake. The inset shows an Eadie-Hofstee transformation of the data. $V_m = 0.63 \pm 0.04 \text{ nmol} \cdot \text{min}^{-1} \cdot \text{mg}^{-1}$, $K_m = 27 \pm 4 \text{ nM Ca}^{2+}$

where S stands for the free Ca^{2+} concentration in the medium and V'_m and K'_m represent the Michaelis-Menten kinetic parameters of a "high affinity" component and V''_m and K''_m those of a "low affinity" component. Data from bepridil inhibition of Na^+ -dependent Ca^{2+} uptake were fitted according to:

$$V = 1 - \{(1 - \beta) \cdot [I]^n / (K_i^n + [I]^n)\} \quad (2)$$

where β stands for the fraction of exchange activity insensitive to bepridil, $[I]$ for the inhibitor concentration, K_i for the apparent half-maximal inhibitor concentration and n for the apparent Hill-coefficient. The data were analyzed with a nonlinear regression data analysis program [22]. Data were analyzed statistically by the Student's t test or the Mann-Whitney U -test, where appropriate. Statistical significance was accepted for $P < 0.05$.

Results

Stripped intestinal mucosa of the tilapia generates a net mucosa to serosa Ca^{2+} flux (Table 2). Ouabain

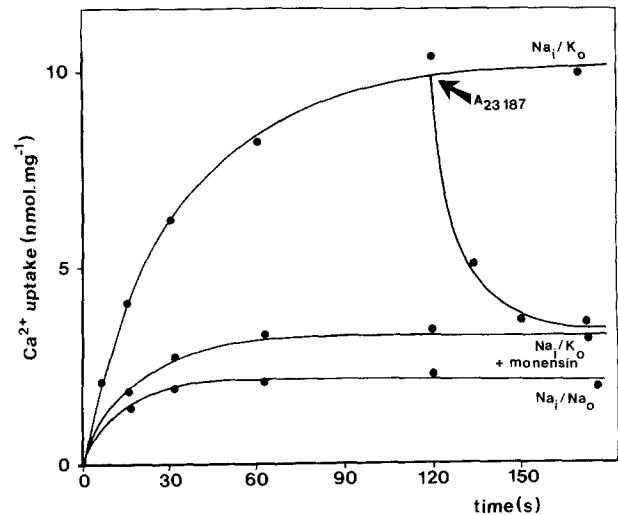


Fig. 2. Sodium-driven Ca^{2+} uptake in basolateral membrane vesicles of tilapia enterocytes. Ca^{2+} uptake in the presence of a 150 mM Na^+ gradient (Na_i/K_o) and $5 \mu\text{M Ca}_o^{2+}$ is reversed by the addition of the Ca^{2+} ionophore A23187, indicating that accumulation of Ca^{2+} occurs. In the presence of the Na^+ ionophore monensin or in the absence of a Na^+ gradient ($\text{Na}_i = \text{Na}_o = 150 \text{ mM}$) Ca^{2+} uptake is greatly diminished. Mean values of one experiment in triplicate are given

added to the serosal side specifically inhibits the mucosa-to-serosa flux by 21%, does not affect serosa-to-mucosa flux and results therefore in a 53% decrease in net Ca^{2+} influx. Replacement of Na^+ with NMG^+ reduces mucosa to serosa flux by 41% and abolishes the inhibitory effect of ouabain. We have taken these observations to be evidence for a partial Na^+ dependence of the Ca^{2+} extrusion step in transcellular mucosa-to-serosa Ca^{2+} transport. The next step was to study ATP- and Na^+ -dependent Ca^{2+} transport systems in enterocyte basolateral plasma membrane vesicles.

Figure 1 shows the Ca^{2+} concentration dependence of ATP-driven Ca^{2+} transport in BLMV's. ATP-driven Ca^{2+} transport, determined as the difference in Ca^{2+} accumulated in 1 min in the presence and in the absence of ATP, obeyed Michaelis-Menten kinetics. A maximum velocity of $0.63 \pm 0.04 \text{ nmol} \cdot \text{min}^{-1} \cdot \text{mg}^{-1}$ and a half-maximal activation concentration for Ca^{2+} of $27 \pm 4 \text{ nM}$ was calculated ($n = 12$). Oxalate (20 mM) did not stimulate ATP-driven Ca^{2+} transport ($V_m = 0.76 \pm 0.14 \text{ nmol} \cdot \text{min}^{-1} \cdot \text{mg}^{-1}$, $K_m = 65 \pm 21 \text{ nM Ca}^{2+}$; $n = 3$), suggesting that our membrane preparation is not significantly contaminated with endoplasmic reticular fragments [23]. Correcting for 29% inside-out resealed vesicles, the maximum velocity rises to $2.17 \text{ nmol} \cdot \text{min}^{-1} \cdot \text{mg}^{-1}$.

Figure 2 shows that an outwardly directed Na^+ gradient drives Ca^{2+} uptake (determined at $5 \mu\text{M Ca}^{2+}$). Addition of the sodium ionophore monensin,

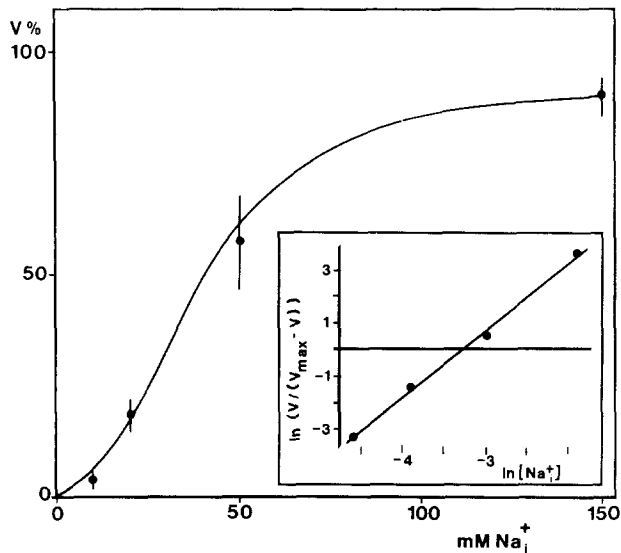


Fig. 3. Na^+ dependence of Na^+ -driven Ca^{2+} uptake. Membrane vesicles were equilibrated in 10, 20, 50 or 150 mM Na^+ . Initial rates (5-sec determinations) of Na^+ -driven Ca^{2+} uptake (Na_i/K_o) were corrected for "non-specific" Ca^{2+} uptake ($K_i = K_o = 150$ mM). The medium Ca^{2+} concentration was $5 \mu\text{M}$. Values for V are expressed relative to V_m , which was $20.3 \pm 4.6 \text{ nmol} \cdot \text{min}^{-1} \cdot \text{mg}^{-1}$ ($n = 3$). The inset shows a Hill-plot of the data; a Hill-coefficient of 2.5 ± 0.2 and a K_m of 38 ± 5 mM Na^+ was derived

which dissipates the Na^+ gradient, reduced Ca^{2+} uptake. True accumulation of Ca^{2+} took place since addition of calcium ionophore A23187 reduced Na^+ -driven Ca^{2+} uptake.

Figure 3 shows the Na^+ concentration dependence of Ca^{2+} uptake by basolateral membrane vesicles. The maximum velocity was $20.3 \pm 4.6 \text{ nmol} \cdot \text{min}^{-1} \cdot \text{mg}^{-1}$ at $5 \mu\text{M}$ Ca^{2+} . A Hill-coefficient for Na^+ of 2.5 ± 0.2 was derived (inset), indicating at least two sites for Na^+ on the $\text{Na}^+/\text{Ca}^{2+}$ exchanger. An apparent half-maximal activation concentration of 38 ± 5 mM Na^+ was calculated.

Figure 4 shows the Ca^{2+} concentration dependence of Na^+ -driven Ca^{2+} uptake. The Eadie-Hofstee plot of the data (inset) demonstrates that this process did not obey simple Michaelis-Menten kinetics. This implies that more than one Ca^{2+} site is involved in the activation of the $\text{Na}^+/\text{Ca}^{2+}$ exchange. When the data were fitted to Eq. (1), the maximum velocity of the Ca^{2+} uptake process with high affinity for Ca^{2+} was $7.2 \pm 2.8 \text{ nmol} \cdot \text{min}^{-1} \cdot \text{mg}^{-1}$ and its K_m was $181 \pm 78 \text{ nM}$ Ca^{2+} ; the respective values for the low affinity component were $32.1 \pm 2.2 \text{ nmol} \cdot \text{min}^{-1} \cdot \text{mg}^{-1}$ and $3.3 \pm 1.1 \mu\text{M}$ Ca^{2+} ($n = 15$). Addition of the K^+ ionophore valinomycin ($9 \mu\text{M}$) stimulated Na_i^+ -dependent Ca^{2+} uptake by $120 \pm 30\%$ ($n = 11$) independent of medium Ca^{2+} concentration (7.5×10^{-5} to 5×10^{-3} mM), indicating electrogenic behavior of the $\text{Na}^+/\text{Ca}^{2+}$ exchanger.

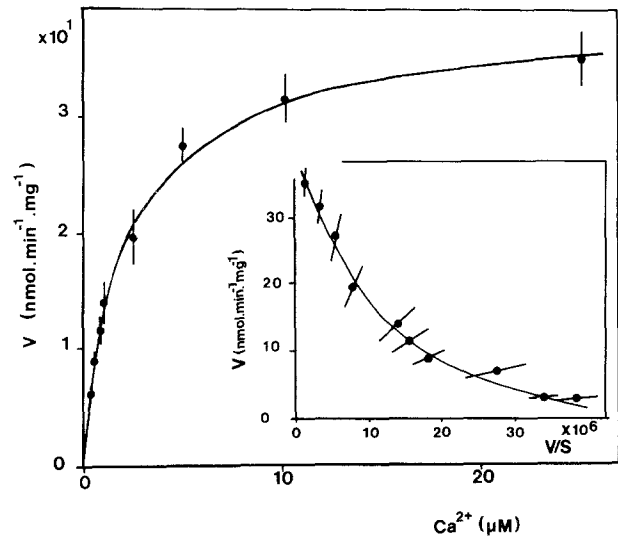


Fig. 4. Ca^{2+} dependence of Na^+ -driven Ca^{2+} uptake. Initial rates of Na^+ -driven Ca^{2+} uptake (Na_i/K_o) were corrected for "non-specific" Ca^{2+} uptake ($\text{Na}_i = \text{Na}_o = 150$ mM). Ca_o^{2+} was varied between 7.5×10^{-5} and 2.5×10^{-2} mM. The inset shows an Eadie-Hofstee transformation of the data. V_m and K_m values are $7.2 \text{ nmol} \cdot \text{min}^{-1} \cdot \text{mg}^{-1}$ and 181 nM Ca^{2+} , respectively, for the high affinity component and $32.1 \text{ nmol} \cdot \text{min}^{-1} \cdot \text{mg}^{-1}$ and $3.3 \mu\text{M}$ Ca^{2+} for the low affinity component ($n = 15$)

Hence, the apparent stoichiometry of the $\text{Na}^+/\text{Ca}^{2+}$ -exchange process appears to be greater than 2 Na^+ to 1 Ca^{2+} .

Recalling that an average 53% of the vesicles in our preparation are resealed and assuming symmetrical behavior of the $\text{Na}^+/\text{Ca}^{2+}$ exchanger [27], the maximum velocity of the $\text{Na}^+/\text{Ca}^{2+}$ -exchange process with high affinity for Ca^{2+} rises to $13.6 \text{ nmol} \cdot \text{min}^{-1} \cdot \text{mg}^{-1}$. Thus the maximum Ca^{2+} transport capacity of the exchange process exceeds the capacity of the $(\text{Ca}^{2+} + \text{Mg}^{2+})$ -ATPase by a factor of 6.27.

The Ca^{2+} entry blocker bepridil [15], when applied to the outside medium only, produced a dose-dependent and partial inhibition of $\text{Na}^+/\text{Ca}^{2+}$ exchange ($\text{Na}_i = 150$ mM, $\text{Ca}_o^{2+} = 1 \mu\text{M}$). The residual, bepridil-insensitive, activity was $44 \pm 3\%$; the K_i was $45 \pm 9 \mu\text{M}$ ($n = 4$). A monophasic Hill-plot was observed and a Hill-coefficient of 1.3 ± 0.2 was derived, indicating one binding site for bepridil (Fig. 5). Bepridil inhibition was noncompetitive with Ca^{2+} (Fig. 6), which follows from the specific effect on the maximum velocity of the exchange process.

Figure 7 summarizes experiments designed to evaluate the relative contribution of $(\text{Ca}^{2+} + \text{Mg}^{2+})$ -ATPase and $\text{Na}^+/\text{Ca}^{2+}$ exchange to Ca^{2+} uptake in basolateral membranes. ATP-driven Ca^{2+} uptake was determined in media containing graded amounts of NaCl in the presence or absence (control) of ouabain. As the ouabain site of the $(\text{Na}^+ + \text{K}^+)$ -ATPase is directed towards the vesicular lu-

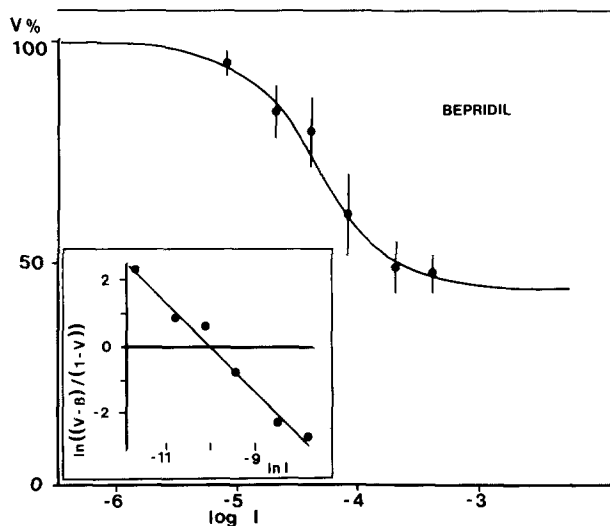


Fig. 5. Dose dependence of bepridil inhibition of $\text{Na}^+/\text{Ca}^{2+}$ exchange in tilapia enterocyte plasma membranes, determined at $\text{Na}_i = 150 \text{ mM}$, $K_o = 150 \text{ mM}$ and $\text{Ca}_o^{2+} = 1 \mu\text{M}$. Initial rates of Ca^{2+} uptake were corrected for "non-specific" uptake ($\text{Na}_i = \text{Na}_o = 150 \text{ mM}$). The residual, bepridil-insensitive, activity was $44 \pm 3\%$. The inset shows a Hill-plot of the data; a Hill-coefficient of 1.3 ± 0.2 and a K_i of $45 \pm 9 \mu\text{M}$ bepridil was derived ($n = 4$)

men in the inside-out vesicles in which ATP-driven Ca^{2+} transport takes place, vesicles were preincubated on ice for 2 hr with 1 mM ouabain. In separate experiments it was ascertained that this treatment fully blocks $(\text{Na}^+ + \text{K}^+)\text{-ATPase}$ activity in the membrane preparation. Ca^{2+} uptake in ouabain-treated vesicles was not affected by Na^+ . In control vesicles, however, Ca^{2+} uptake was progressively stimulated (up to 100%) with Na^+ concentrations increasing up to 15 mM. At higher Na^+ concentrations (up to 50 mM) the stimulation of Ca^{2+} uptake decreased again, but remained elevated above the uptake in the presence of ouabain. The increase in stimulation of vesicular Ca^{2+} uptake by Na^+ appeared the strongest around the K_m values for Na^+ (9 mM) of the $(\text{Na}^+ + \text{K}^+)\text{-ATPase}$ activity in the membrane preparation (Fig. 7, inset).

Discussion

We conclude from the data presented that Ca^{2+} absorption in the intestine of freshwater tilapia is Na^+ dependent and that a $\text{Na}^+/\text{Ca}^{2+}$ exchange system in the basolateral plasma membrane of the enterocyte may contribute substantially to the active extrusion of Ca^{2+} from cell to blood. The strong correlation between Na^+ -dependent, ouabain-sensitive trans-epithelial Ca^{2+} transport and the presence of a high

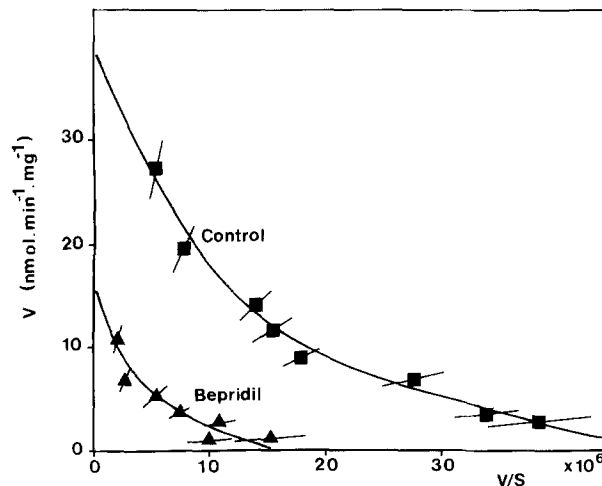


Fig. 6. Effects of bepridil ($80 \mu\text{M}$) on the Ca^{2+} kinetics of $\text{Na}^+/\text{Ca}^{2+}$ exchange in tilapia enterocyte plasma membranes. Inhibition proved noncompetitive for Ca^{2+} as indicated by the specific effects on the maximum velocities of the exchange process ($n = 3-15$)

affinity and high capacity $\text{Na}^+/\text{Ca}^{2+}$ exchange in the basolateral membrane of the enterocyte in the fish intestine was not found for the mammalian intestine [16].

SODIUM DEPENDENCE OF Ca^{2+} ABSORPTION

To our knowledge this is the first study reporting net unidirectional Ca^{2+} fluxes across intestinal mucosa of a freshwater fish. The data indicate a potential role for fish intestine in whole body Ca^{2+} homeostasis. No comparable studies on intestinal mucosa of other fish species are known to us. The close correspondence of the mucosa-to-serosa flux in the absence of sodium (with or without ouabain present) and the serosa-to-mucosa flux under control conditions and in the presence of ouabain suggests that the serosa-to-mucosa flux is paracellular and that removing sodium completely abolished the transcellular active movement of Ca^{2+} . We attribute the Na^+ dependence of Ca^{2+} absorption by the fish intestine to a dependence on the $\text{Na}^+/\text{K}^+\text{-ATPase}$ activity in the basolateral plasma membranes of the enterocyte. The ouabain sensitivity of the mucosa-to-serosa Ca^{2+} flux is in line with this contention. The partial inhibition of the transcellular Ca^{2+} transport by ouabain could have resulted from an incomplete collapse of the electrochemical sodium potential. We found, however, that the mucosa-to-serosa flux decreased in the first 15-min period after addition of ouabain to a level that remained stable for

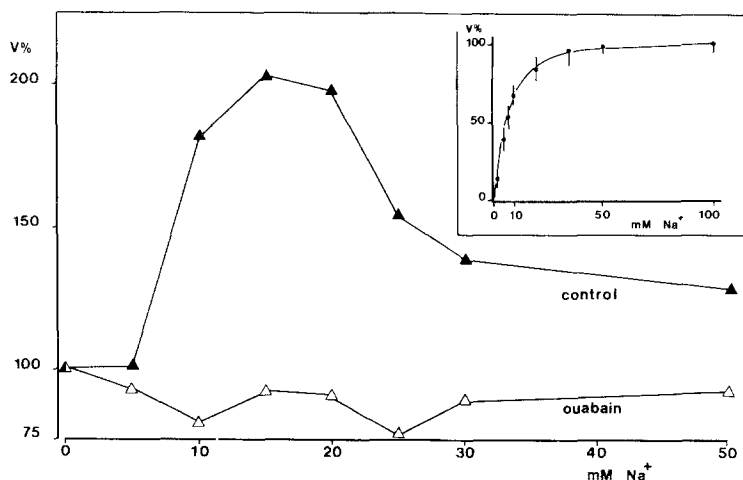


Fig. 7. ATP-dependent and Na^+ gradient-dependent Ca^{2+} uptake in tilapia enterocyte plasma membrane vesicles. Initial rates (1-min determinations) of ATP-dependent Ca^{2+} uptake were corrected for ATP-independent uptake. The Na^+ concentration in the medium was varied between 0 and 50 mM, the Ca^{2+} concentration in the medium was 5 μM . ($\text{Na}^+ + \text{K}^+$)-ATPase activity was blocked by a 2-hr preincubation of vesicles on ice with 1 mM ouabain. Under ouabain inhibition, ATP-driven Ca^{2+} uptake is not affected by Na^+ . In the absence of ouabain (when Na^+ will be accumulated in inside-out oriented vesicles as a result of ($\text{Na}^+ + \text{K}^+$)-ATPase activity and hence a Na^+ gradient will be created) Ca^{2+} uptake doubled around K_m values for Na^+ (9 mM) of the ($\text{Na}^+ + \text{K}^+$)-ATPase in these membranes (inset, $n = 3$). Ca^{2+} uptake at 0 mM Na^+ was designated 100%. Mean values for two experiments in triplicate are given.

the following 30 min. If the electrochemical potential for Na^+ indeed drives most of the net Ca^{2+} transport, this suggests that the largest drop in the Na^+ potential occurs in the first minutes after ouabain addition. This reasoning is in concordance with membrane potential and sodium content measurements in goldfish (*Carassius auratus*) intestine [1, 18]. In pilot experiments we observed large fluctuations in fluxes after about 1 hr in the presence of ouabain. Therefore, we restricted the experimental time to 45 min. We tentatively conclude that ouabain does not completely abolish transcellular movement of Ca^{2+} and that the residual net flux of Ca^{2+} in the presence of ouabain results from Ca^{2+} extrusion mediated through Ca^{2+} -ATPase activity.

Proceeding from an intestinal surface of 50 cm^2 in a 250-g tilapia for the first 30 cm intestine that we used in our studies, we calculated an intestinal Ca^{2+} uptake capacity from our in vitro data (Table 1) of 1.7 $\mu\text{mol} \cdot \text{hr}^{-1}$. The branchial Ca^{2+} uptake for the same fish is calculated to be 3.6 $\mu\text{mol} \cdot \text{hr}^{-1}$ [9]. The numbers indicate the potential importance of the intestine for Ca^{2+} uptake in freshwater fish. This notion is in line with observations by Berg [4] on freshwater goldfish. These fish increase their intestinal calcium absorption in soft waters with decreased availability of Ca^{2+} in the water for branchial uptake. A more direct demonstration of the involvement of a $\text{Na}^+/\text{Ca}^{2+}$ exchanger in trans-epithelial Ca^{2+} transport awaits the development of more specific inhibitors. Bepridil (see below) is suitable to use as an inhibitor of $\text{Na}^+/\text{Ca}^{2+}$ exchange in

vitro [15, and this study], but its side effects on, e.g., ATPase activities [39] and on Ca^{2+} channels [35] make the substance inappropriate for studies in intact tissue.

ATP-ENERGIZED Ca^{2+} TRANSPORT

The demonstration of an ATP-dependent Ca^{2+} transporter in the fish enterocyte plasma membrane, although unprecedented, could have been anticipated for a Ca^{2+} transporting epithelium (in fact for any cell) and extends our observations on similar Ca^{2+} transport mechanisms in fish gills [11–14, 26]. However, we were surprised by the low apparent transport capacity derived for the ATP-energized Ca^{2+} pump. The low capacity cannot be explained by artifacts introduced by the isolation procedure. A 2.5% recovery and a 9.3-fold purification of the plasma membrane marker Na^+/K^+ -ATPase are congruent with data previously published by us [26, 37] and by others [3, 16, 19] on a variety of Ca^{2+} transporting epithelia. One could argue that a loss of calmodulin during the isolation procedure resulted in the low V_m observed. However, the high affinity for Ca^{2+} *per se* is indicative of the presence of calmodulin in the preparation [14, 38]. Moreover, addition of extra calmodulin to the membranes did not affect the kinetics of the Ca^{2+} transport (*data not shown*) and this observation is consistent with similar data on Ca^{2+} transport in fish gill plasma membranes [14, 37]. Furthermore, the

numbers for resealing and inside-out orientation do not deviate from previously published data on comparable membrane preparations from fish [14] and mammalian tissues [16, 19]. We conclude therefore that the tilapia enterocyte plasma membrane has a low density of ATP-dependent calcium pumps. An attractive hypothesis is that the low density of Ca^{2+} pumps in the fish enterocyte is apparently compensated for by a Na^+ -dependent Ca^{2+} extrusion system. This is consistent with the high $(\text{Na}^+ + \text{K}^+)\text{-ATPase}$ content of the enterocytes and the presence of a plasma membrane bound $\text{Na}^+/\text{Ca}^{2+}$ exchanger with kinetic parameters favorable to Ca^{2+} extrusion.

Na^+ -DEPENDENT Ca^{2+} TRANSPORT

The $\text{Na}^+/\text{Ca}^{2+}$ exchange activity in the plasma membrane of tilapia enterocytes resembles similar exchangers in plasma membranes of e.g., rat intestine [16, 20], kidney cortex [19, 21], dog red blood cells [25], cardiac sarcolemma [27–31], bovine retinal rod outer segments [6] or in *Artemia* membranes [5]. First, since valinomycin stimulates $\text{Na}^+/\text{Ca}^{2+}$ exchange in membrane vesicles ($\text{Na}_i^+ = 150 \text{ mM}$, $K_o^+ = 150 \text{ mM}$), the $\text{Na}^+/\text{Ca}^{2+}$ exchanger appears to be electrogenic and transports therefore more than two Na^+ ions per Ca^{2+} ion. Second, bepridil inhibits the $\text{Na}^+/\text{Ca}^{2+}$ exchange activity partially (56%) and noncompetitively for Ca^{2+} . Our results on bepridil inhibition of $\text{Na}^+/\text{Ca}^{2+}$ exchange corroborate in all aspects the data of Garcia et al. [15], who investigated the mechanism of inhibition by bepridil of $\text{Na}^+/\text{Ca}^{2+}$ exchange in porcine sarcolemma. Third, the $\text{Na}^+/\text{Ca}^{2+}$ exchange activity is located in the plasma membrane, where it is co-located with ouabain-sensitive $(\text{Na}^+ + \text{K}^+)\text{-ATPase}$ and ATP-driven Ca^{2+} pump activities (see Fig. 7). Fourth, data on vesicle Ca^{2+} uptake determined under conditions that allow the controlled and simultaneous operation of the ATP-driven Ca^{2+} pump and the $\text{Na}^+/\text{Ca}^{2+}$ exchanger provide direct evidence in vitro for a significant contribution of the exchanger to Ca^{2+} extrusion across the plasma membrane (see Fig. 7). However, we cannot exclude that the kinetic properties of the ATPase and the exchanger are influenced by the isolation procedure, which may affect the relative contribution of either carrier to Ca^{2+} transport and allows only a tentative extrapolation to their activities in the intact cell.

A not fully apprehended result is that Ca^{2+} dependence of $\text{Na}^+/\text{Ca}^{2+}$ exchange turned out to be biphasic (showing a high affinity and a low affinity site for Ca^{2+}). This biphasic response to Ca^{2+} could have derived from the occurrence of different cell populations (e.g., crypt *vs.* villus) in intestinal mu-

cosa. However, in contrast to mammalian intestines, where villus cells and crypt cells each present a characteristic molecular make-up [7], tilapia intestine provides a more simple and homogeneously folded mucosa without crypts. More relevant is our observation that $\text{Na}^+/\text{Ca}^{2+}$ exchange determined in canine erythrocyte membrane vesicles shows a similar biphasic Ca^{2+} dependence (*unpublished*). Apparently this phenomenon has a more general occurrence.

The biphasic response to the medium Ca^{2+} concentration was demonstrated by using Ca^{2+} buffers in the assay medium, which allows the precise definition of concentrations below $50 \mu\text{M}$ Ca^{2+} . Many reports on $\text{Na}^+/\text{Ca}^{2+}$ exchange (irrespective of the tissue or species investigated) have evaluated only the effects of Ca^{2+} concentrations above $50 \mu\text{M}$, or do not report the use of Ca^{2+} buffer systems. Therefore, exchange activity with a high affinity for Ca^{2+} may have gone undetected in many studies. However, there is a report by Gill, Chueh and Whitlow [17], in which the Ca^{2+} dependence of $\text{Na}^+/\text{Ca}^{2+}$ exchange in rat cerebral synaptosomes was studied using an assay system including Ca^{2+} buffers. These authors also found a biphasic dependence on Ca^{2+} of the exchanger. A high affinity for Ca^{2+} in the submicromolar range (0.3 to $0.8 \mu\text{M}$ Ca^{2+}) was derived. Unfortunately the low affinity component of their exchange activity proved unsaturable with Ca^{2+} and this prevented complete analysis of maximum velocities of the carrier. The question remains however, whether the biphasic behavior indicates the presence of two carriers or may be attributed to a single carrier with a Ca^{2+} concentration-defined affinity for Ca^{2+} . Bepridil inhibited, albeit partially, $\text{Na}^+/\text{Ca}^{2+}$ exchange independently of Ca^{2+} concentration. Our data on bepridil inhibition do not allow the distinction of two carriers with different bepridil sensitivities. Gill and coworkers [17] came to a similar conclusion evaluating the effects of the less potent drug amiloride (which in analogy to bepridil is assumed to interact with a sodium site [34]) on synaptosomal $\text{Na}^+/\text{Ca}^{2+}$ exchange.

We realize that fitting our kinetic data of the $\text{Na}^+/\text{Ca}^{2+}$ exchanger to the sum of two separate saturable processes suggests the existence of separate biochemical entities. We emphasize that this fit was only used to describe our data reproducibly. To our knowledge there are at the moment no reports on probes for the Ca^{2+} site(s) of the $\text{Na}^+/\text{Ca}^{2+}$ exchanger that would allow specific (pharmacological) discrimination of classes of Ca^{2+} sites on the molecule as indicated by our kinetic studies. However, Cd^{2+} may prove a useful tool for this purpose, as its interaction with the Ca^{2+} site of the Ca^{2+} pumping ATPase was shown to be highly specific [38]. Experiments on the interaction of Cd^{2+} with $\text{Na}^+/\text{Ca}^{2+}$

exchange are presently being carried out. For the complex Ca²⁺ dependence of the Na⁺/Ca²⁺ exchange process an important analogy may well exist with the kinetic behavior of the gramicidin ion channel. The profile of the dependence of the conductance of this ion channel upon ion activity is well represented by a biphasic Eadie-Hofstee plot, if one assumes two interacting sites for the permeant ion (as was shown to be realistic for Cs⁺, Rb⁺, K⁺ and H⁺ conductance of valine-gramicidin A in artificial bilayers [8, 32]). An attractive hypothesis that arises from our data is that the enterocyte Na⁺/Ca²⁺ exchanger has two interacting Ca²⁺ sites. At low calcium concentrations the Na⁺/Ca²⁺ exchanger displays high affinity for Ca²⁺ and this allows involvement of Na⁺/Ca²⁺ exchange in the extrusion of cytosolic calcium.

The authors thank Klaas Dekker for skillful assistance in the flux experiments, Mr. Peter Klaren for assistance in transport studies and Tom Spanings for excellent organization of fish husbandry. T.J.M. Schoenmakers is supported by the Foundation for Fundamental Biological Research (BION), which is subsidized by the Netherlands Organization for Scientific Research (NWO).

References

1. Albus, H., Groot, J.A., Siegenbeek van Heukelom, J. 1979. Effects of glucose and ouabain on transepithelial electrical resistance and cell volume in stripped and unstripped goldfish intestine. *Pfluegers Arch.* **383**:55–66
2. Bakker, R., Groot, J.A. 1984. cAMP-mediated effects of ouabain and theophylline on paracellular ion selectivity. *Am. J. Physiol.* **246**:G213–G217
3. Bayerdörffer, E., Haase, W., Schulz, I. 1985. Na⁺/Ca²⁺ countertransport in plasma membrane of rat pancreatic acinar cells. *J. Membrane Biol.* **87**:107–119
4. Berg, A. 1970. Studies on the metabolism of calcium and strontium in freshwater fish. II. Relative contribution of direct and intestinal absorption in growth conditions. *Mem. Ist. Ital. Idrobiol. Dott Marco de Marchi* **26**:241–255
5. Cheon, J., Reeves, J.P. 1988. Sodium-calcium exchange in membrane vesicles from *Artemia*. *Arch. Biochem. Biophys.* **267**:736–741
6. Cook, N.J., Kaupp, U.B. 1988. Solubilization, purification, and reconstitution of the sodium-calcium exchanger from bovine retinal rod outer segments. *J. Biol. Chem.* **263**:11382–11388
7. Corven, E.J.J.M., Roche, C., Van Os, C.H. 1985. Distribution of Ca²⁺-ATPase, ATP-dependent Ca²⁺ transport, calmodulin and vitamin D-dependent Ca²⁺ binding protein along the villus-crypt axis in rat duodenum. *Biochim. Biophys. Acta* **820**:274–282
8. Eisenmann, G., Sandblom, J., Neher, E. 1978. Interactions in cation permeation through the gramicidin channel. Cs, Rb, K, Na, Li, Tl, H and effects of anion binding. *Biophys. J.* **22**:307–340
9. Favus, M.J., Angeid-Backman, E., Breyer, M.D., Coe, F.L. 1983. Effects of trifluoperazine, ouabain and ethacrynic acid on intestinal calcium transport. *Am. J. Physiol.* **244**:G111–G115
10. Flik, G., Fenwick, J.C., Kolar, Z., Mayer-Gostan, N., Wendelaar Bonga, S.E. 1985a. Whole-body calcium flux rates in cichlid teleost fish *Oreochromis mossambicus* adapted to freshwater. *Am. J. Physiol.* **249**:R432–R437
11. Flik, G., Fenwick, J.C., Wendelaar Bonga, S.E. 1989. Calcitropic actions of prolactin in freshwater North American eel (*Anguilla rostrata* LeSueur). *Am. J. Physiol.* **257**:R74–R79
12. Flik, G., Perry, S.F. 1989. Cortisol stimulates whole body calcium uptake and the branchial calcium pump in freshwater rainbow trout. *J. Endocrinol.* **120**:75–82
13. Flik, G., Van Rijs, J.H., Wendelaar Bonga, S.E. 1985b. Evidence for high-affinity Ca²⁺-ATPase activity and ATP-driven Ca²⁺-transport in membrane preparations of the gill epithelium of the cichlid fish *Oreochromis mossambicus*. *J. Exp. Biol.* **119**:335–347
14. Flik, G., Wendelaar Bonga, S.E., Fenwick, J.C. 1985c. Active Ca²⁺ transport in plasma membranes of branchial epithelium of the North-American eel, *Anguilla rostrata* LeSueur. *Biol. Cell.* **55**:265–272
15. Garcia, M.L., Slaughter, R.S., King, V.F., Kaczorowski, G.J. 1988. Inhibition of sodium-calcium exchange in cardiac sarcolemmal membrane vesicles. 2. Mechanism of inhibition by bepridil. *Biochemistry* **27**:2410–2415
16. Ghijsen, W.E.J.M., De Jong, M.D., Van Os, C.H. 1983. Kinetic properties of Na⁺/Ca²⁺ exchange in basolateral plasma membranes of rat small intestine. *Biochim. Biophys. Acta* **730**:85–94
17. Gill, D.L., Chueh, S-H., Whitlow, C.L. 1984. Functional importance of the synaptic plasma membrane calcium pump and sodium-calcium exchanger. *J. Biol. Chem.* **259**:10807–10813
18. Groot, J.A., Albus, H., Bakker, R. 1981. Analysis of the ouabain induced increase in transepithelial electrical resistance in the goldfish intestinal mucosa. *Pfluegers Arch.* **392**:67–71
19. Heeswijk, M.P.M. van, Geertsen, J.A.M., Os, C.H. van 1984. Kinetic properties of the ATP-dependent Ca²⁺ pump and the Na⁺/Ca²⁺ exchange system in basolateral membranes from rat kidney cortex. *J. Membrane Biol.* **79**:19–31
20. Hildmann, B., Schmidt, A., Murer, H. 1982. Ca²⁺-transport across basal-lateral plasma membranes from rat small intestinal epithelial cells. *J. Membrane Biol.* **65**:55–62
21. Jayakumar, A., Cheng, L., Liang, C.T., Sacktor, B. 1984. Sodium gradient-dependent calcium uptake in renal basolateral membrane vesicles. *J. Biol. Chem.* **259**:10827–10833
22. Leatherbarrow, R.J. 1987. A non-linear regression analysis program for the IBM PC. Elsevier Biosoft, Amsterdam
23. Moore, L., Fitzpatrick, D.F., Chen, T.S., Landon, E.J. 1974. Calcium pump activity of the renal plasma membrane and renal microsomes. *Biochim. Biophys. Acta* **345**:405–418
24. Murer, H., Hildmann, B. 1981. Transcellular transport of calcium and inorganic phosphate in the small intestinal epithelium. *Am. J. Physiol.* **240**:G409–G416
25. Ortiz, O.E., Sjodin, R.A. 1984. Sodium- and adenosine-triphosphate-dependent calcium movements in membrane vesicles prepared from dog erythrocytes. *J. Physiol. (London)* **354**:287–301
26. Perry, S.F., Flik, G. 1988. Characterization of branchial transepithelial calcium fluxes in freshwater trout, *Salmo gairdneri*. *Am. J. Physiol.* **254**:R491–R498
27. Philipson, K.D. 1985. Symmetry properties of the Na⁺-Ca²⁺ exchange mechanism in cardiac sarcolemmal vesicles. *Biochim. Biophys. Acta* **821**:367–376
28. Philipson, K.D., Nishimoto, A.Y. 1982. Na⁺-Ca²⁺ exchange

- in inside-out cardiac sarcolemmal vesicles. *J. Biol. Chem.* **257**:5111–5117
29. Philipson, K.D., Ward, R. 1986. Ca^{2+} transport capacity of sarcolemmal $\text{Na}^+/\text{Ca}^{2+}$ exchange. Extrapolation of vesicle data to in vivo conditions. *J. Mol. Cell. Cardiol.* **18**:943–951
 30. Reeves, J. P., Hale, C. C. 1984. The stoichiometry of the cardiac sodium-calcium exchange system. *J. Biol. Chem.* **259**:7733–7739
 31. Reeves, J.P., Sutko, J.L. 1983. Competitive interactions of sodium and calcium with the sodium-calcium exchange system of cardiac sarcolemmal vesicles. *J. Biol. Chem.* **258**:3178–3182
 32. Sandblom, J., Eisenman, G., Neher, E. 1977. Ionic selectivity, saturation and block in gramicidin A channels: I. Theory for the electrical properties of ion selective channels having two pairs of binding sites and multiple conductance states. *J. Membrane Biol.* **31**:383–417
 33. Sillen, L.G., Martell, A.E. 1964. Stability constants of metal ion complexes. The Chemical Society, Special Publication no. 17, London
 34. Slaughter, R.S., Garcia, M.L., Cragoe, E.J., Jr., Reeves, J.P., Kaczorowski, G.J. 1988. Inhibition of sodium-calcium exchange in cardiac sarcolemmal membrane vesicles. I. Mechanism of inhibition by amiloride analogues. *Biochemistry* **27**:2403–2409
 35. Spedding, M. 1985. Activators and inactivators of Ca^{2+} channels: New perspectives. *J. Pharmacol. (Paris)* **16**:319–343
 36. Van Os, C.H. 1987. Transcellular calcium transport in intestinal and renal epithelial cells. *Biochim. Biophys. Acta* **906**:195–222
 37. Verboost P.M., Flik, G., Lock, R.A.C., Bonga, S.E.W. 1988. Cadmium inhibits plasma membrane calcium transport. *J. Membrane Biol.* **102**:97–104
 38. Verboost, P.M., Flik, G., Pang, P.K.T., Lock, R.A.C., Wendelaar Bonga, S.E. 1989. Cadmium inhibition of the erythrocyte Ca^{2+} pump. A molecular interpretation. *J. Biol. Chem.* **264**:5613–5615
 39. Younes, A., Fontanarava, C., Schneider, J.M. 1981. Effects of bepridil on the Ca^{2+} dependent ATPase activity of sarcoplasmic reticulum. *Biochem. Pharmacol.* **30**:2979–2981

Received 28 March 1989; revised 9 August 1989